


Review

Grid Connection Circuits for Powerful Regenerative Electric Drives of Rolling Mills: Review

Alexander S. Maklakov ^{1,*}, Tao Jing ² , Alexander A. Nikolaev ^{1,3} and Vadim R. Gasiyarov ⁴ ¹ Research & Innovation Services, South Ural State University, 454080 Chelyabinsk, Russia² School of Mechanical and Electrical Engineering, China Jiliang University, Hangzhou 310018, China³ Department of Automated Electric Drives and Mechatronics, Nosov Magnitogorsk State Technical University, 455000 Magnitogorsk, Russia⁴ Department of Automated Control Systems, Nosov Magnitogorsk State Technical University, 455000 Magnitogorsk, Russia

* Correspondence: alexandr.maklakov.ru@ieee.org

Abstract: AC regenerative electric drives (AC REDs) are widely used in metallurgical rolling due to their reliability, efficiency, and power sufficient to maintain the process. This paper reviews the latest achievements in building the grid connection circuits for the main AC REDs of rolling mills. The paper discusses multipulse connection circuits formed by various transformer types and algorithms for preprogrammed pulse-width modulation with selective harmonic elimination technique (PPWM with SHE) of three-level active front ends (AFE), provides the theoretical and practical measurement results, and gives recommendations for improving existing systems. For 6-, 12-, and 18-pulse grid connection circuits, switching patterns of AFE semiconductor modules with a smooth downward trend within the modulation index range from 0.7 to 1.15 are provided. A simulation was performed under comparable conditions on simulation models in the Matlab/Simulink to objectively evaluate the performance and opportunities of 6-, 12-, and 18-pulse grid connection circuits, including the three-level AFE and transformer specifications. The waveforms and spectra of the grid currents and transformer secondary winding phase currents are shown; total harmonic distortion (THD) factors have been calculated up to the 60th harmonic for various PPWM with SHE patterns. The results of simulation and experimental measurement on operating equipment have been compared. The paper is expected to provide a broad overview of multipulse connection circuits of the rolling mill's main AC REDs, in particular, identify the latest solutions capable of significantly improving their electromagnetic compatibility with the grid. The results obtained are of high genericity and can be used by researchers and engineers to provide the electromagnetic compatibility of non-linear consumers in similar circuits, as well as design them.

Keywords: power converters; electric drive; pulse width modulation; voltage quality; multipulse connection circuits



Citation: Maklakov, A.S.; Jing, T.; Nikolaev, A.A.; Gasiyarov, V.R. Grid Connection Circuits for Powerful Regenerative Electric Drives of Rolling Mills: Review. *Energies* **2022**, *15*, 8608. <https://doi.org/10.3390/en15228608>

Academic Editor: Amin Mahmoudi

Received: 31 August 2022

Accepted: 15 November 2022

Published: 17 November 2022

Publisher's Note: MDPI stays neutral with regard to jurisdictional claims in published maps and institutional affiliations.



Copyright: © 2022 by the authors. Licensee MDPI, Basel, Switzerland. This article is an open access article distributed under the terms and conditions of the Creative Commons Attribution (CC BY) license (<https://creativecommons.org/licenses/by/4.0/>).

1. Introduction

The sustainable development of energy-saving industrial technologies has led to the widespread use of power conversion systems capable of recovering electrical energy for high-power applications. Until the middle of the 20th century, they were based on semi-controlled thyristor converters to adjust AC and DC electric drives. From the middle of the 20th century to this day, they were replaced by fully controlled multilevel converters based on transistors or gated thyristors (Figure 1). To date, almost all modern metallurgical rolling mill electric drives are based on synchronous or asynchronous AC motors and, as a rule, active front ends as part of frequency converters [1–4].

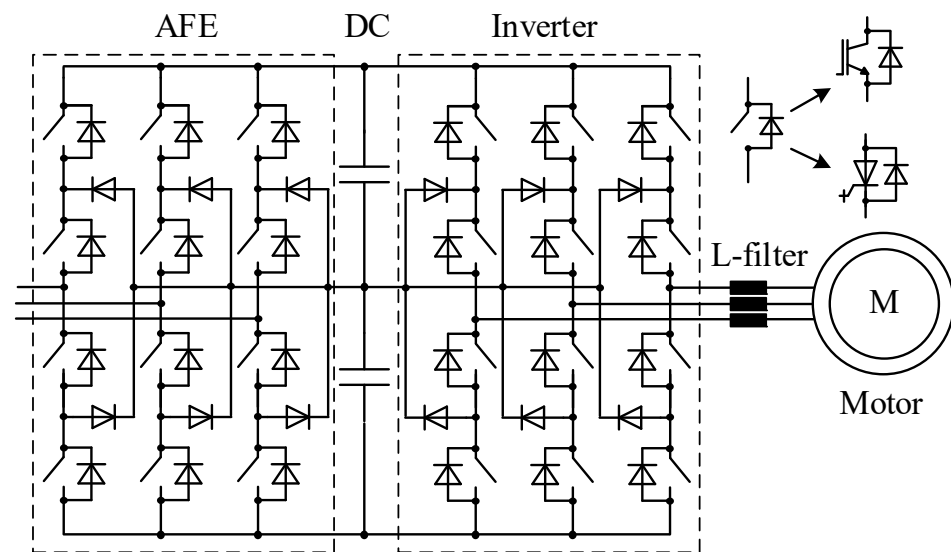


Figure 1. Regenerative electric drives of rolling mills.

A device called an active front-end (AFE) has several common names found in the scientific and technical literature: PWM boost rectifier, voltage source rectifier, grid-connected voltage source inverter, regenerative rectifier, and bidirectional converter. Semiconductor AFE modules are switched using various pulse-width modulation (PWM) algorithms, which results in a non-sinusoidal output AC voltage and thus makes it challenging to provide electromagnetic compatibility for the consumer and the source. Due to these problems, standards and guidelines [5–8] have been introduced for the equipment manufacturers and users to rely on. If the feed transformer's secondary winding inductance is not enough to maintain stable AFE operation, then passive L or LC filters should be additionally installed in existing systems on the grid side. However, the specifications of these filters are close to those of the frequency converter, which increases not only their cost but also the losses and the number of components, deteriorating the system reliability. Active or hybrid filters have not gained popularity in the systems under consideration [9–13].

Switching losses and electromagnetic compatibility with the grid are the most significant problems for the main AC regenerative electric drives (AC REDs) of rolling mills with AFEs, whose rated power reaches tens of megawatts. They cause overheating or complete failure of electronic equipment at the common grid connection point. Researchers and experts have developed various ways and techniques to reduce the impact of these problems [14–18].

A well-known approach to improving the quality of power converted by semiconductor converters is developing multilevel topologies. Multilevel converter manufacturers recommend them to control powerful electrical energy consumers from tens to hundreds of megawatts [19–22]. However, it turned out that an increase in the converter's output voltage also increases the number of semiconductor components, thereby reducing the converter reliability and efficiency. Among all multilevel topologies, the three-level neutral-point-clamped (NPC) topology [23], shown in Figure 2, is the most common and compromised solution. The NPC converter's total DC link voltage U_{dc} is shared between the DC link equivalent capacitances C_1, C_2 in equal proportion. The converter's positive and negative input voltage U_{an} is generated when current flows through two series-connected semiconductor modules S_{1a}, S_{2a} or $\bar{S}_{1a}, \bar{S}_{2a}$, which can be either fully controlled switches or diodes. The zero (third) level of the PWM converted voltage U_{an} is generated when current flows through fully controllable switches S_{1a} or \bar{S}_{2a} and clamping diodes D_{1a} or D_{2a} .

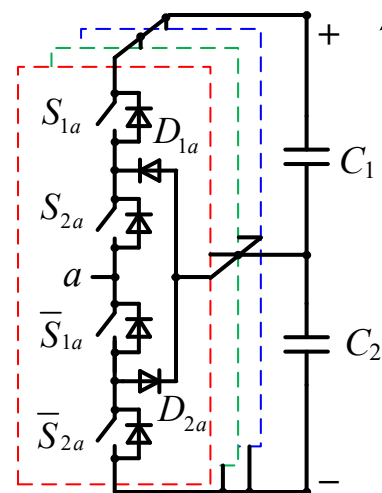


Figure 2. Phase leg of a three-level NPC converter.

The next way to reduce the negative impact of semiconductor converters is to choose the optimal PWM algorithm. The analysis of quite a few of scientific papers and production runs determined preprogrammed PWM (PPWM) as the primary PWM technique for AFEs as part of the rolling mill's main AC RED frequency converters. The PPWM algorithms switch semiconductor AFE modules according to precalculated switching sequences, generating an internal AFE PWM voltage with the required quality. Since its inception, PPWM has aroused great research interest for controlling semiconductor switches of high-power AFEs at low frequencies within 150–450 Hz. The low switching capacity is determined by the limited semiconductor base opportunities for the rated power above 1 MW. An increase in the switching frequency causes overheating of the semiconductor modules, which, as a result, requires additional heavy-duty cooling, significantly reducing the converter efficiency and reliability [24–26].

The last effective technique for reducing the negative impact of power semiconductor converters on the power quality, in particular, the total harmonic distortion (THD) and the voltage and current individual harmonic factors, is multipulse grid connection circuits. Multipulse circuits solve two important problems at once: they increase a rate power and improve electromagnetic compatibility. Transformers are the key multipulse circuit components. In 2007, Singh et al. [27] comprehensively reviewed multipulse circuits covering a lot of transformer configurations. In 2020, Jie Chen et al. [28] updated this review, focusing on the application of multi-winding transformer-based grid connection circuits in various aircraft types. However, the primary focus of the published review papers was only on low-power unidirectional converters based on diode rectifiers and already obsolete bidirectional thyristor ones. Many of the considered technical solutions are not used for power circuits connecting the main AC REDs of rolling mills to the grid. Currently, it seems more important not to consider the benefits of a particular multipulse connection circuit or multi-winding transformer but rather study several factors related to the choice of converter topology, PWM techniques, and power system parameters at once. The scientific literature fails to pay enough attention to such comprehensive studies.

The paper's key objective is to review the latest achievements in building grid connection circuits for the main AC REDs of rolling mills. The paper describes 6-, 12-, and 18-pulse grid connection circuits and technologies applicable to these solutions. Sixty publications [1–60] were analyzed in the field of topology for building high-power PWM converters, techniques, and algorithms and multipulse connection circuits. Despite the focus on only the circuits used in the AC REDs as the key study objective, its results are also suitable for other adjustable speed drive systems, static var compensators, flexible AC systems, and HVDC transmission lines. The results obtained are of high genericity and

can be used by researchers and engineers to provide the electromagnetic compatibility of non-linear consumers in similar circuits and design them.

The paper is arranged in a conventional way. The introduction describes the research object, shows the study's relevance, and formulates goals and problems. Section 2 describes the most common power circuits of the main AC REDs of rolling mills. Section 3 considers and discusses the algorithms of PPWM with SHE for 6-, 12-, and 18-pulse grid connection circuits. Section 4 provides the simulation results. Section 5 is devoted to demonstrating the production run results. Section 6 provides the conclusion.

2. Power Circuits of the Main Electric Drives of Rolling Mills

This section will firstly consider six-pulse circuits shown in Figure 3 and used for the main electric drives of the bar and the 1700 cold rolling mills. They are the simplest ones and consist of a single-winding transformer, a bidirectional frequency converter with AFE built according to a three-level neutral-point-clamped NPC topology, an output L-filter, and an AC drive motor [29–33]. The transformer windings have zero shift between primary and secondary voltages and are star/star (Figure 3a) or delta/delta (Figure 3b) connected. The six-pulse circuit has significant individual current harmonic factors $6n \pm 1$ (n is any positive integer). PPWM with a frequency of 350 Hz is generally used for AFE, but with heavy-duty cooling, it can be increased up to 450 Hz. Table 1 provides the key specifications of the considered connection circuit.

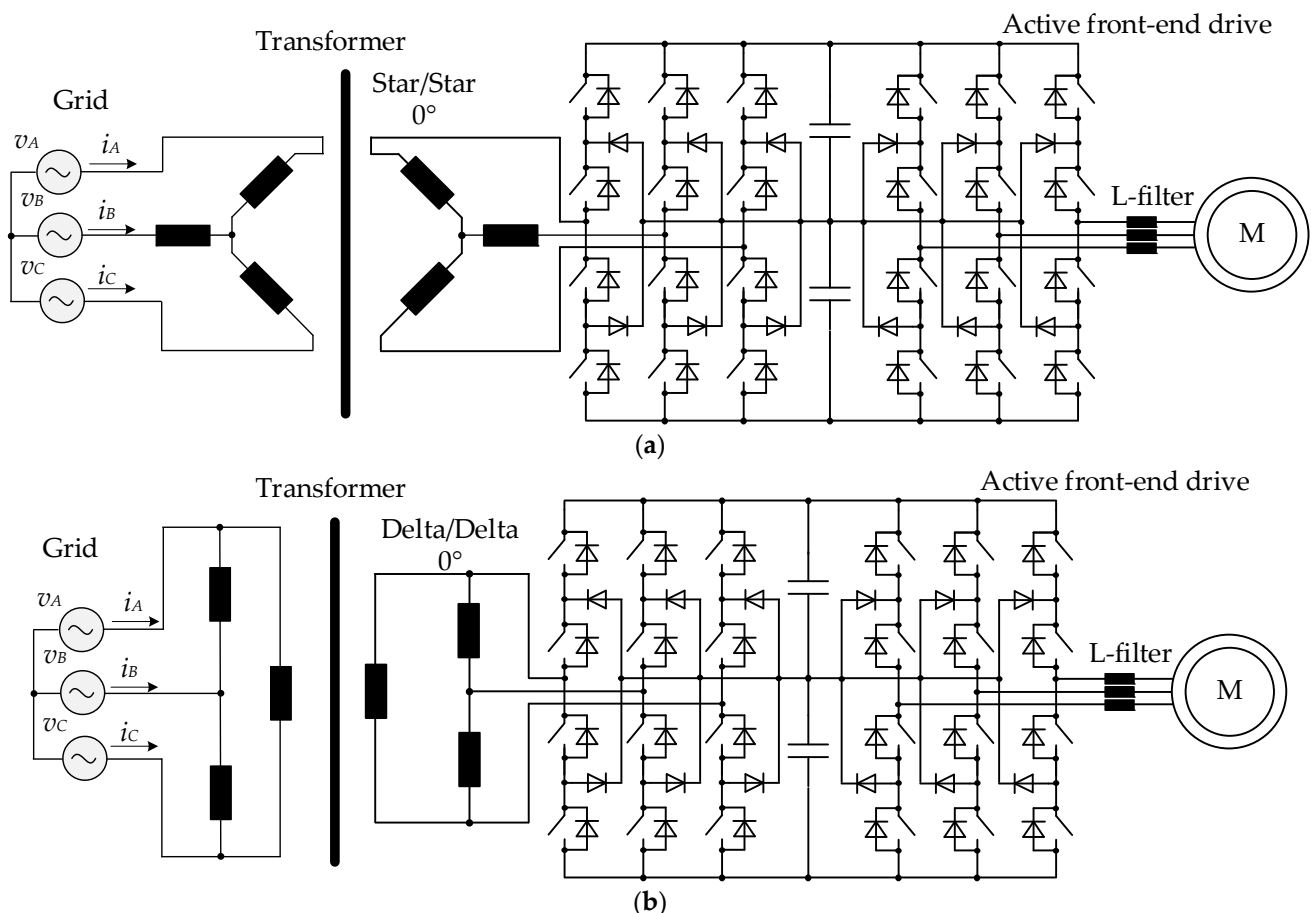


Figure 3. Six-pulse circuits for connecting the main AC REDs of rolling mills to the grid: (a) cold-rolling mill; (b) Bar mill.

Twelve-pulse circuits are the next most common ones. Figure 4 shows the grid connection circuits of the main electric drives of the 2000 cold and the 1750 hot rolling mills. The 12-pulse circuit has only significant individual current harmonic factors $12n \pm 1$. This is

achieved through the use of a net-side phase-shift transformer with a series connection of primary windings [34–37]. One secondary winding of such a transformer is star-connected and another is delta-connected, thereby shifting the secondary voltage by 30° . The secondary windings are connected to separate AFEs operating with PPWM at a frequency of 250–350 Hz. The major requirement for harmonic mitigation in a 12-pulse circuit is a balanced load of two AFEs. In this case, the AFE-generated harmonic factors $12n \pm 1$ will have the same amplitude and mitigate in the transformer. This reduces the requirements for additional current filtering compared to the six-pulse circuit. Note the following circuit characteristics (see Figure 4): (1) in the transformer's two independent magnetic systems, a 30° phase shift of secondary voltages occurs, which allows reducing power losses in the magnetic core; (2) two frequency converters have a combined DC link, which allows maintaining a given level in the common DC bus when the transistors of one AFE are turned off; (3) the series connection of the primary phase-shifting transformer windings allows for equally separated the grid voltage between them. Table 1 provides the key circuit specifications.

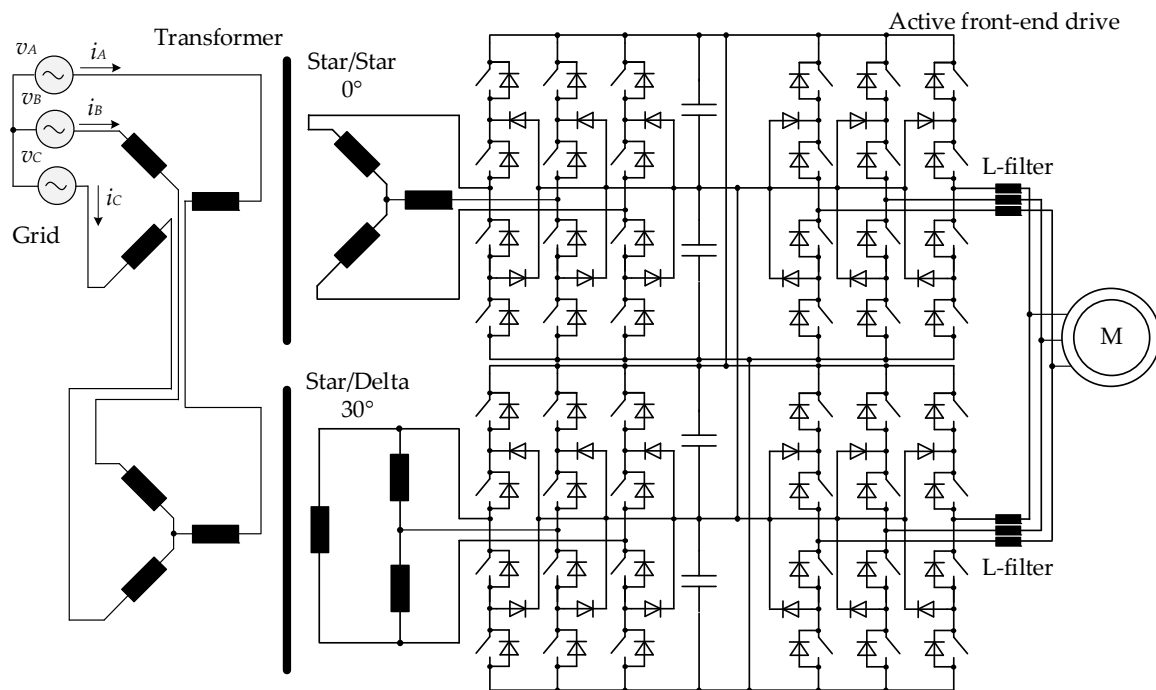


Figure 4. Twelve-pulse connection circuit based on a net-side phase-shift transformer with series connection of primary windings.

Figure 5 shows 12-pulse circuits, which can also be found in the metallurgical rolling [38–41]. The circuit in Figure 5a is based on a single multi-winding transformer, the secondary windings of which are connected to two AFEs with a 30° shift. The transformer's unified magnetic system with additional losses in the magnetically conductive steel due to mixing harmonic components is a significant drawback of this circuit compared to that in Figure 4. Another version of the 12-pulse circuit in Figure 5b is based on two single-winding transformers connected in parallel, the secondary windings of which are connected to two AFEs. This circuit has another significant drawback compared to the previous ones, i.e., higher transformer cost, larger weight, and size parameters.

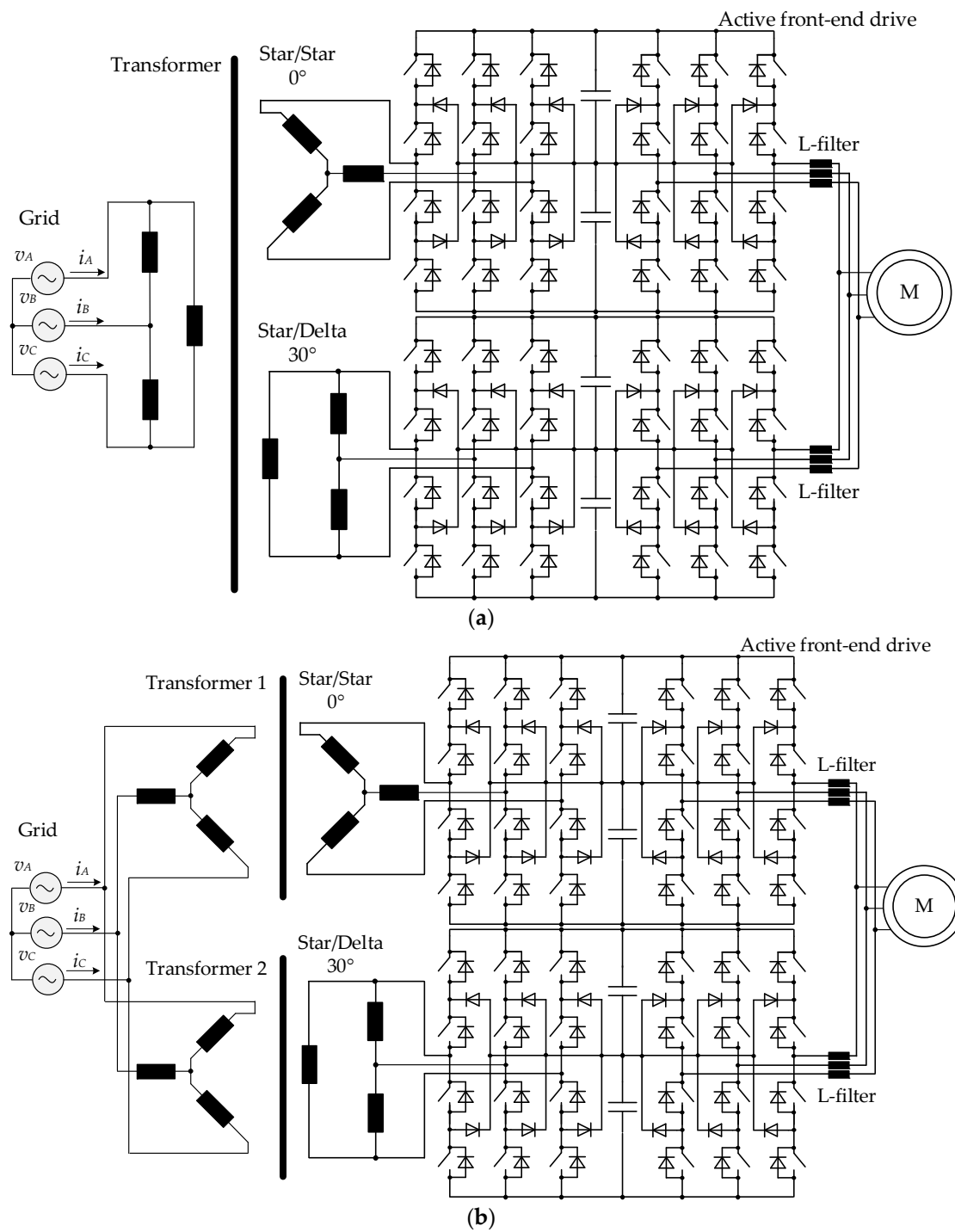


Figure 5. Twelve-pulse circuits based on: (a) Multi-winding phase-shifting transformer; (b) two single-winding transformers connected in parallel.

The last widely spread option in the list is the 18-pulse connection circuit. It is exemplified in Figure 6 by the main electric drive of the 5000 hot rolling mill. The 18-pulse circuit is based on three transformers with 0° , 20° , and -20° phase shifts, connected in parallel, which allows mitigating all current harmonic factors except for $18n \pm 1$ [42–46]. Therefore, 18-pulse circuits have a better quality of the consumed grid current than 6- and 12-pulse ones. The secondary windings of the 18-pulse circuit transformers are connected to three AFEs operating with PPWM at a frequency of 250 Hz. The first harmonic primary voltage vectors are shifted by $\pm 20^\circ$ relative to the secondary ones by the polygonal connection of

the transformers' primary windings while dividing them into two sections providing these sections are electrically connected, and additional phase magnetic fluxes are oppositely directed. The ratio between the primary winding sections is as follows: 65 and 35% of the total turn number falls, respectively, on the larger and smaller parts. Full harmonics mitigation in the 18-pulse circuit is only possible with a balanced load of three AFEs. Compared to 6- and 12-pulse circuits, the requirements to additional filtering are further reduced. Table 1 provides the key specifications of the circuit in Figure 6, and its characteristics are as follows: (1) independent magnetic systems of three transformers allow reducing losses in the magnetic circuits; (2) the electric drive can keep working for some time with two of the three AFEs.

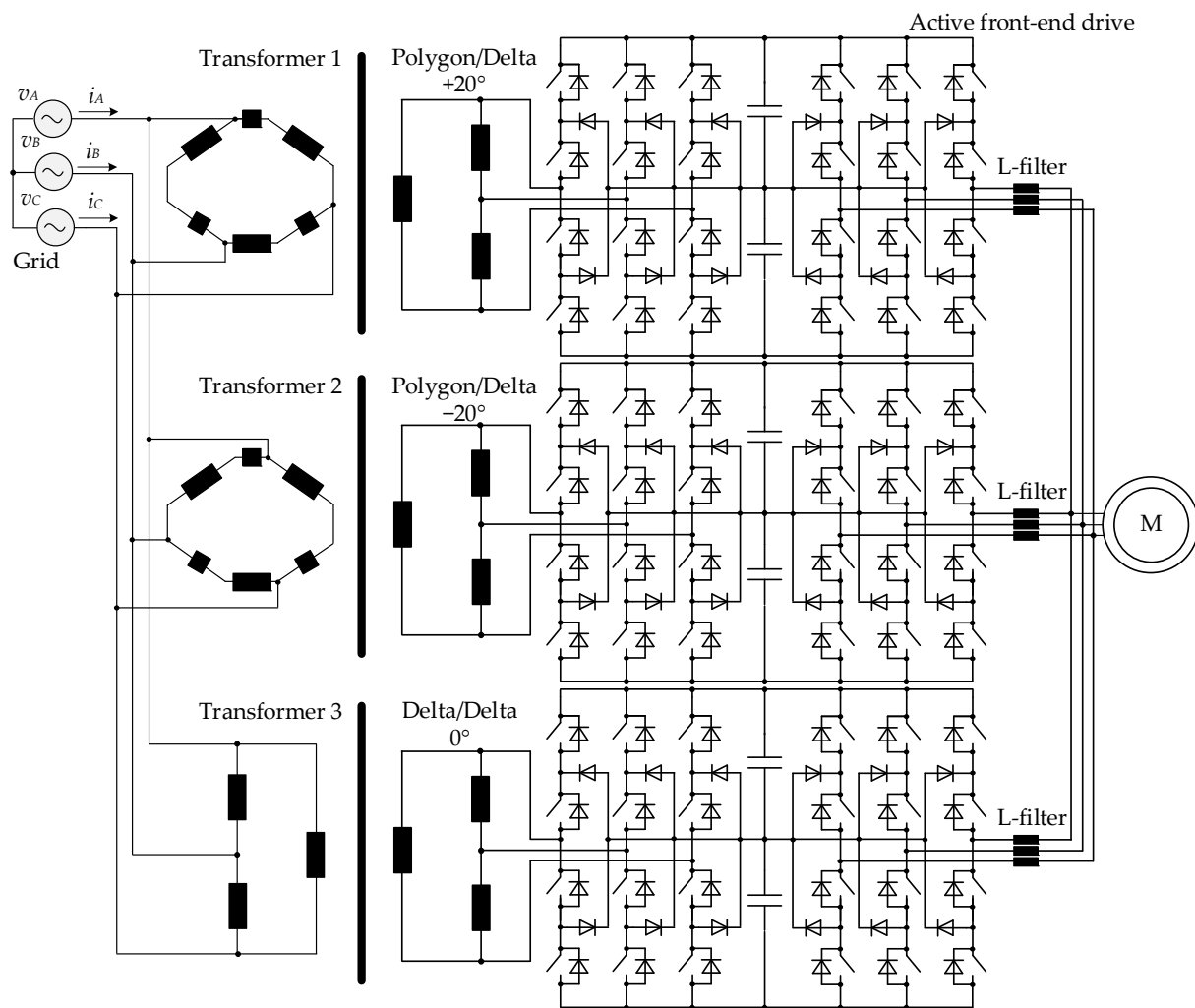


Figure 6. Eighteen-pulse grid connection circuit based on three transformers connected in parallel.

Figure 7 shows the 18-pulse connection circuit for the main electric drives of the 2000 cold-rolling mill. Table 1 provides the key connection circuit specifications. This 18-pulse circuit is based on a multi-winding phase-shift transformer with a series connection of primary windings. The $\pm 20^\circ$ shift of the transformer's secondary voltages is formed by their zigzag connection. Note the following characteristics of the circuit in Figure 7: (1) a single combined DC link is used to power four electric drives at once by connecting to several voltage inverters while providing the 18-pulse circuit powers each motor; (2) the phase-shifting transformer primary windings connected in series allow equally distributing the grid voltage between them.

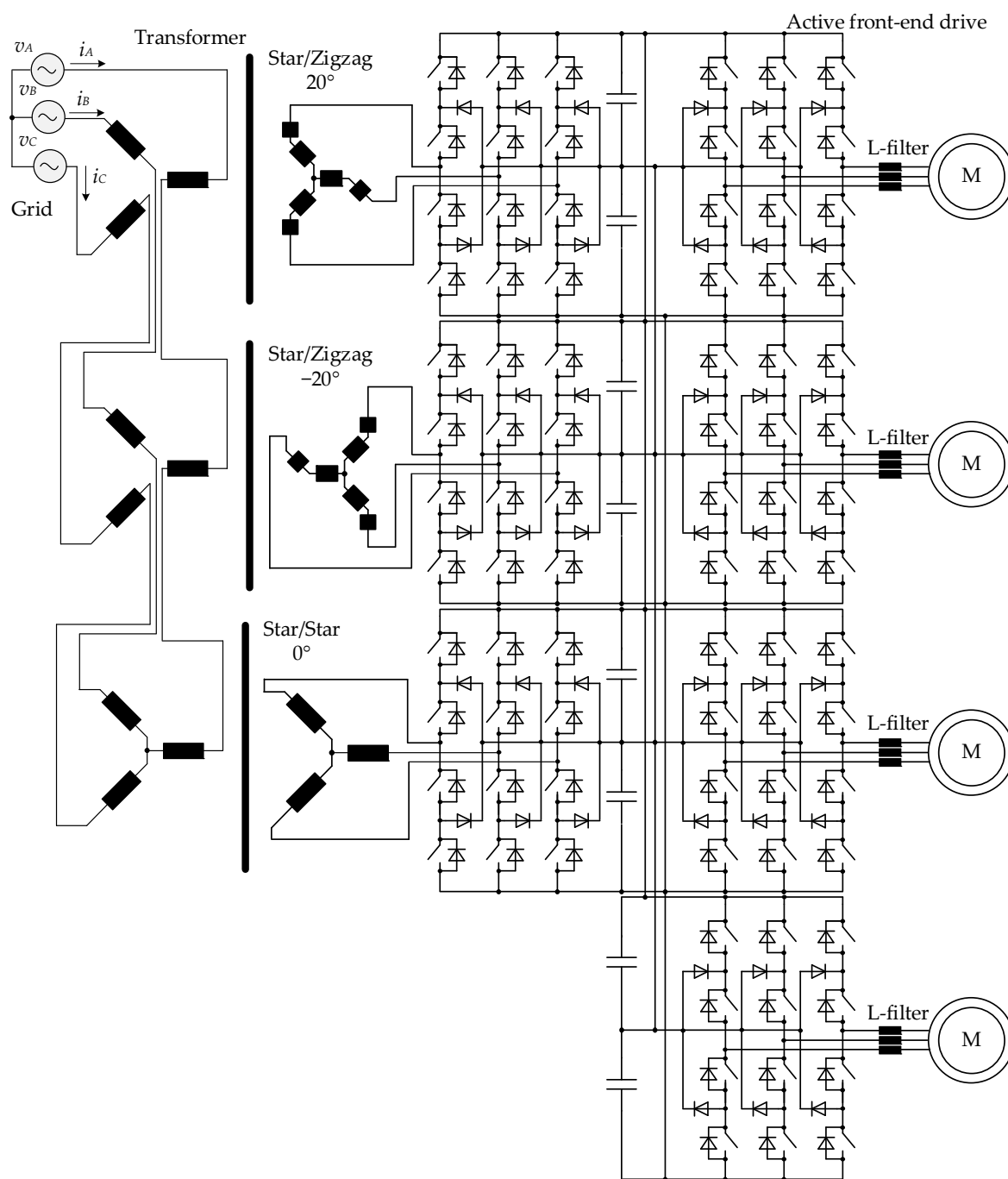


Figure 7. Eighteen-pulse grid connection circuit for the main electric drive of the 2000 cold-rolling mill based on a multi-winding phase-shift transformer with series connection of primary windings.

Table 1. Key specifications of the grid connecting circuits of the main AC RED of rolling mills.

Figure Number	AFE Drive Power S_{AFE} , kVAR	Transformer Power S_T , kVAR	Connection	1st/2nd Transformer Voltage, kV	PPWM Average Frequency
Figure 3a	12,000	12,000	star/star	10/3.3	250–350
Figure 3b	14,000	14,000	delta/delta		
Figures 4 and 5	12,000	12,000	star/delta-star		
Figure 6	18,000	20,000	delta/delta;		
Figure 7	18,000	18,000	delta/double polygon		
			star/delta-double zigzag		

3. PPWM with SHE

It is known that the converted voltage quality of semiconductor converters is primarily determined by the PWM algorithm. An analysis of the scientific and technical literature and experimental data obtained on operating equipment has determined the PPWM with selective harmonic elimination (PPWM with SHE) technique as the major one for three-level AFEs as part of frequency converters for the main AC REDs of rolling mills. PPWM with SHE is particularly efficient at a low switching frequency as part of multipulse circuits. In PPWM with SHE, semiconductor AFE modules are switched according to preprogrammed switching sequences depending on the required converter voltage spectrum, from which harmonics most adversely affecting the current quality are completely eliminated [47–50].

PPWM with SHE algorithms switch semiconductor converter modules at predetermined time instants using N number of precalculated switching angles $\alpha_1, \alpha_2, \dots, \alpha_N$ per quarter of the period (under the condition of quarter-wave symmetry) of the PWM converted voltage within the range from 0 to $\pi/2$, where $0 < \alpha_1 < \alpha_2 < \dots < \alpha_N < \pi/2$. The output voltage waveform allows equating the constant component, even harmonics, and sinusoidal factors of odd harmonics to zero when expanded into a Fourier series and writing the mathematical equation for the PWM converted voltage of a three-level AFE as follows

$$u(\omega t) = \sum_{n=1,3,5,\dots}^{\infty} \left(\frac{4}{n\pi} \left[\sum_{k=1}^N (-1)^{k+1} \cos(n\alpha_k) \right] \cdot \sin(n\omega t) \right), \quad (1)$$

where N is the switching angle number; k is the switching angle serial number from 1 to N . The maximum number of switching angles N can be defined as

$$N = \frac{f_{swave}}{f}, \quad (2)$$

where f_{swave} is the average frequency of PWM with SHE; f is the three-level AFE PWM converted voltage frequency.

The equation determining the relationship between the switching angles and the harmonic spectrum of three-level AFE PWM converted voltage has the form

$$\begin{cases} U_1 = \sum_{k=1}^N (-1)^{k+1} \cdot \cos(\alpha_k) = \frac{\pi}{4} \cdot M \\ U_n = \frac{\pi}{4} \cdot \sum_{k=1}^N (-1)^{k+1} \cdot \cos(n \cdot \alpha_k) = 0 \end{cases} \quad (3)$$

where $n = 5, 7, 11, \dots$; U_1 is the fundamental harmonic level; U_n is the n -th harmonic level; M is the modulation index in the interval $[0, \frac{4}{\pi}]$.

The system (3) successful solution largely depends on the correct choice of the numerical solution method and setting the initial conditions (switching angles) [56–60]. To find the latter, the following equations are used

$$\begin{cases} \alpha_{2k-1}^0 = 30^\circ + 120^\circ \cdot k / (N + 1) - \Delta\alpha \\ \alpha_{2k}^0 = 30^\circ + 120^\circ \cdot k / (N + 1) + \Delta\alpha \\ \alpha_N^0 = 90^\circ - \Delta\alpha \end{cases} \quad (4)$$

where N is the number of switching angles; $k = 1, 2, \dots, (N - 1)/2$ is the switching angle serial number; $\Delta\alpha = 0, \dots, 10$ is the initial mismatch of switching angles to achieve the best solution results.

By Equation (4) for the aforementioned 6-, 12-, and 18-pulse grid connection circuits, the initial conditions, given in Table 2, and switching patterns of semiconductor modules with a smooth downward trend, shown in Figure 8, were calculated within the modulation index range from 0.7 to 1.15.

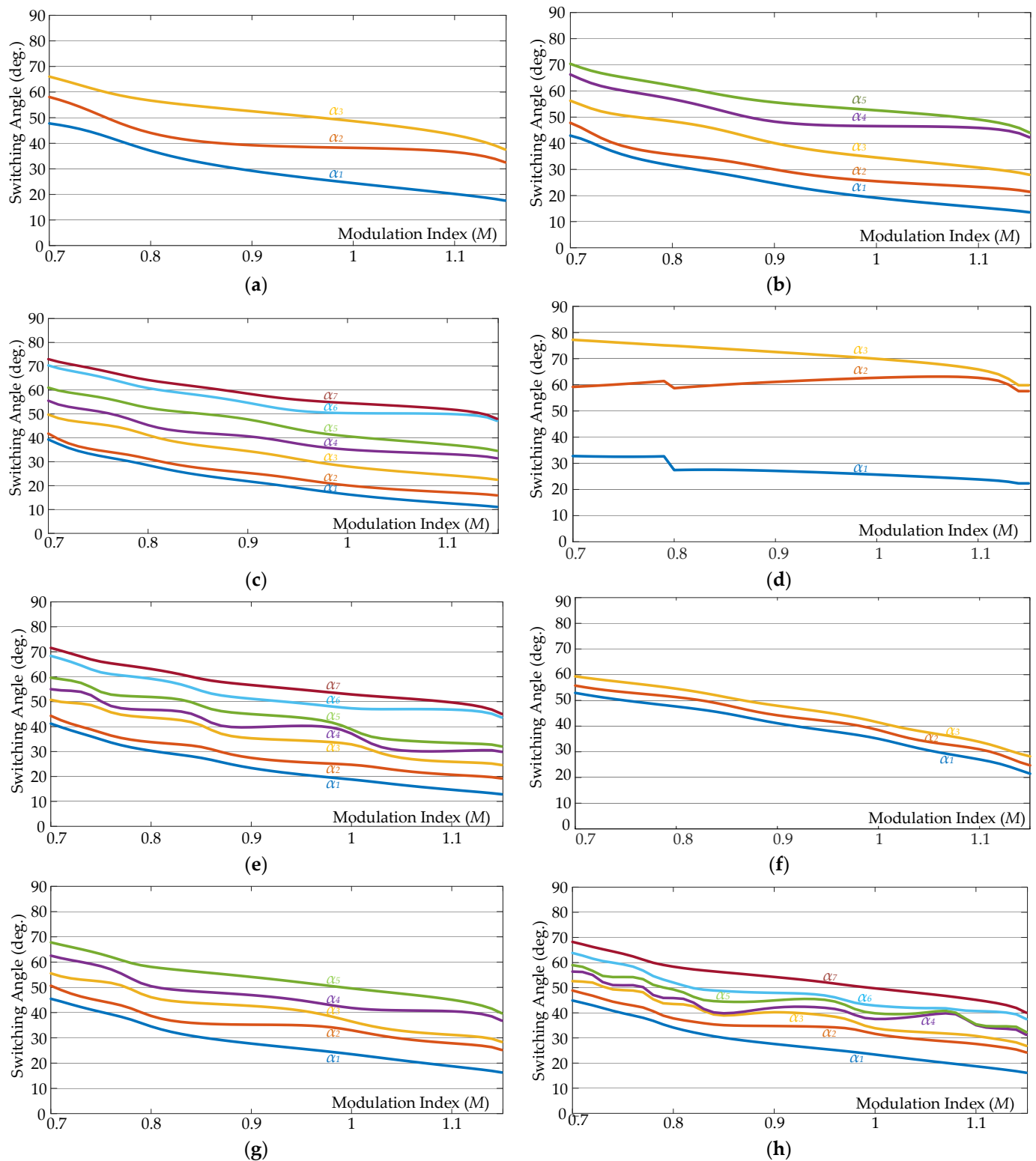


Figure 8. PPWM switching patterns for 6-, 12-, and 18-pulses connection circuits with SHE: (a) 5 and 7; (b) 5, 7, 11, and 13; (c) 5, 7, 11, 13, 17, and 19; (d) 11 and 13; (e) 5, 7, 11, 13, 23, and 25; (f) 17 and 19; (g) 5, 7, 17, and 19; and (h) 5, 7, 17, 19, 35, and 37.

Table 2. The initial switching angle calculation results for 6-, 12-, and 18-pulse circuits.

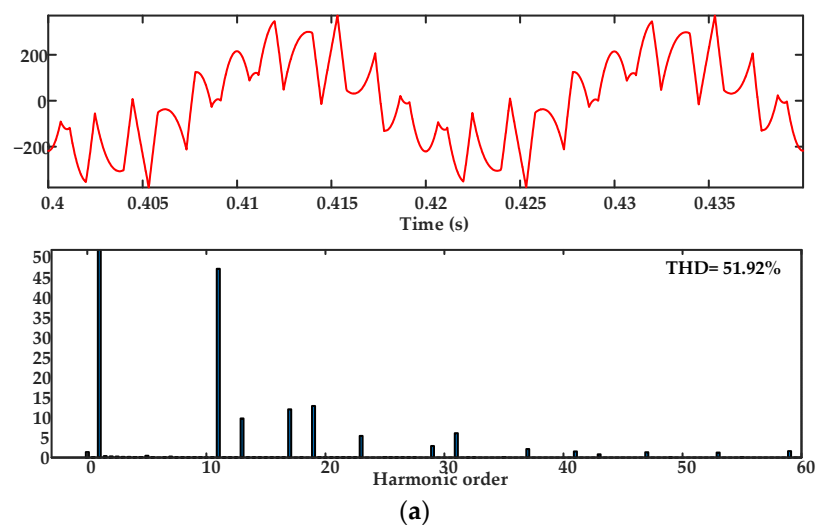
Connection	Figure Number	Eliminated Harmonics	Initial Angles						
			α_1	α_2	α_3	α_4	α_5	α_6	α_7
6—pulse	Figure 8a	5 and 7	59.7	60.3	89.7				
	Figure 8b	5, 7, 11, and 13	49.7	50.3	69.7	70.3	89.7		
	Figure 8c	5, 7, 11, 13, 17, and 19	44.7	45.3	59.7	60.3	74.7	75.3	89.7
12—pulse	Figure 8d	11 and 13	35	55	80				
	Figure 8b	5, 7, 11, and 13	65.5	66.5	77.5	78.5	89.5		
	Figure 8e	5, 7, 11, 13, 23, and 25	53.5	54.5	65.5	66.5	77.5	78.5	89.5
18—pulse	Figure 8f	17 and 19	74.7	75.3	89.6				
	Figure 8g	5, 7, 17, and 19	59.7	60.3	74.7	75.3	89.7		
	Figure 8h	5, 7, 17, 19, 35, and 37	55.2	56.2	63.8	64.8	72.3	73.3	89.5

4. Simulation Results

The analysis of the transformer's primary and secondary winding currents is of interest in terms of comparing the impacts 6-, 12-, and 18-pulse circuits have on the grid. For the sake of direct and proper comparison, simulation was performed with the same AFE rated power, transformer's primary and secondary winding resistance, grid parameters, modulation indices, and the patterns of PPWM with SHE, shown in Figure 8. The simulation was conducted for the circuit power consumption of 2 MW, the grid voltage of 10 kV with a frequency of 50 Hz, the DC voltage of 5020 V, and the modulation index of 1.05. The simulation transformers parameters are shown in Table 3, where U_{sc} is an impedance voltage. The phase currents of the grid and the transformer's secondary winding with a harmonic spectrum are shown in Figures 9–15 and the THD values up to the 60th harmonic component are recorded in Table 4.

Table 3. Transformers parameters.

Grid Connection	S , kVAR	U_1 , V	U_2 , V	I_1 , A	I_2 , A	U_{sc} , %
6-pulse (Figure 3a)	12,000	10,000	3300	693	2189	16
12-pulse (Figure 4)	12,000	10,000	3300	638	1099	14.6
18-pulse (Figure 7)	12,000	10,000	3300	689	675	15

**Figure 9.** Cont.

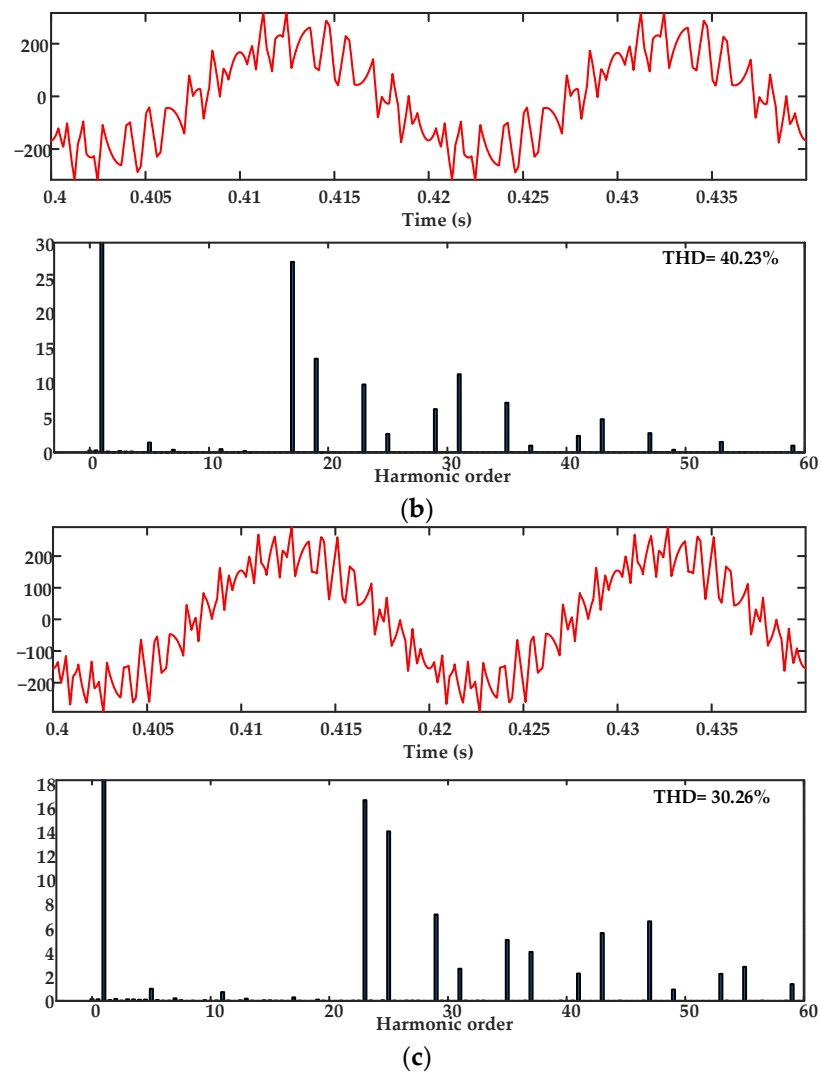


Figure 9. Phase current waveform with harmonic spectrum and THD for 6-pulse connection circuit at PPWM with SHE: (a) 5 and 7; (b) 5, 7, 11, and 13; (c) 5, 7, 11, 13, 17, and 19.

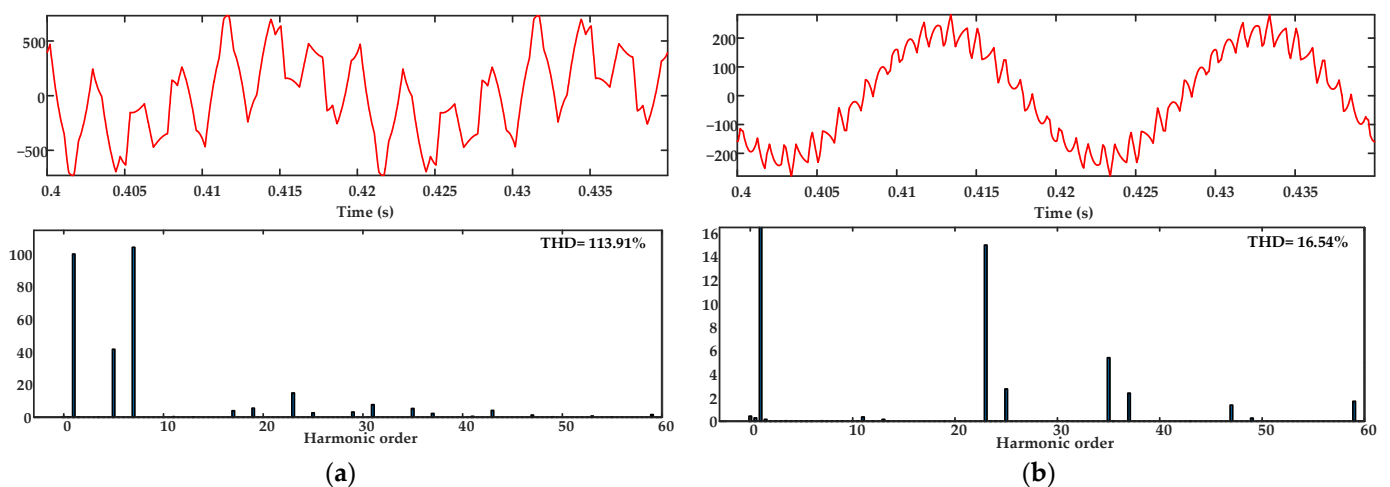


Figure 10. Simulating the current waveform and spectrum in a 12-pulse connection circuit at PPWM with SHE with the 11th and 13th harmonics eliminated: (a) the transformer's secondary winding; (b) Grid.

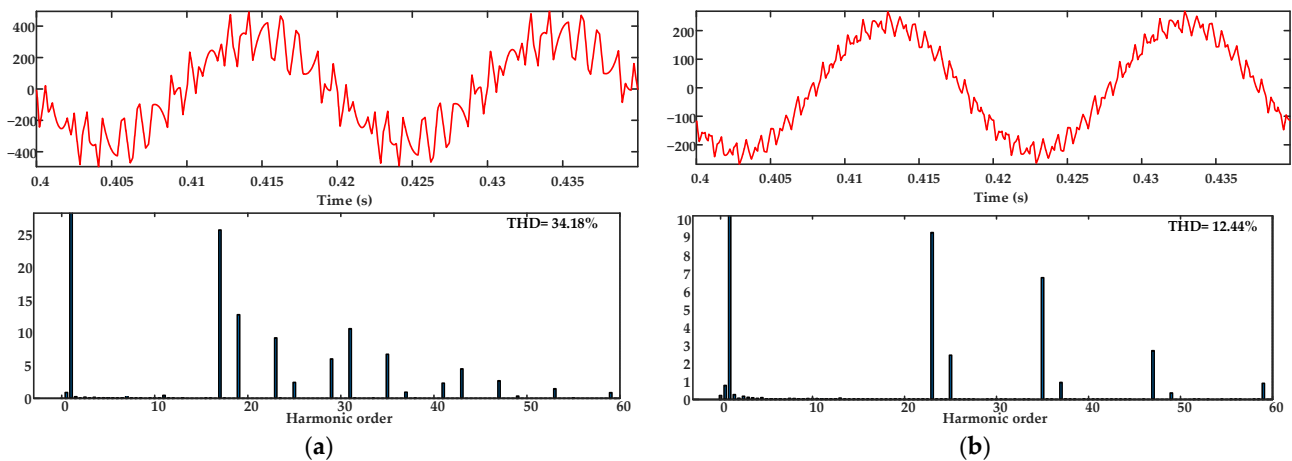


Figure 11. Simulating the current waveform and spectrum in a 12-pulse connection circuit at PPWM with SHE with the 5th, 7th, 11th, and 13th harmonics eliminated: (a) the transformer's secondary winding; (b) grid.

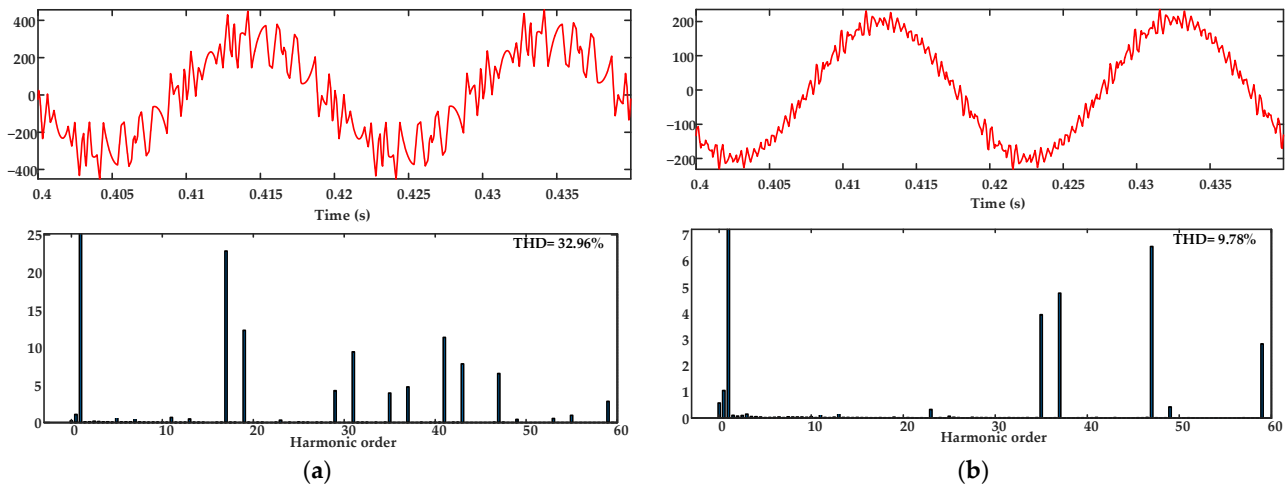


Figure 12. Simulating the current waveform and spectrum in a 12-pulse connection circuit at PPWM with SHE with the 5th, 7th, 11th, 13th, and 23rd harmonics eliminated: (a) the transformer's secondary winding; (b) grid.

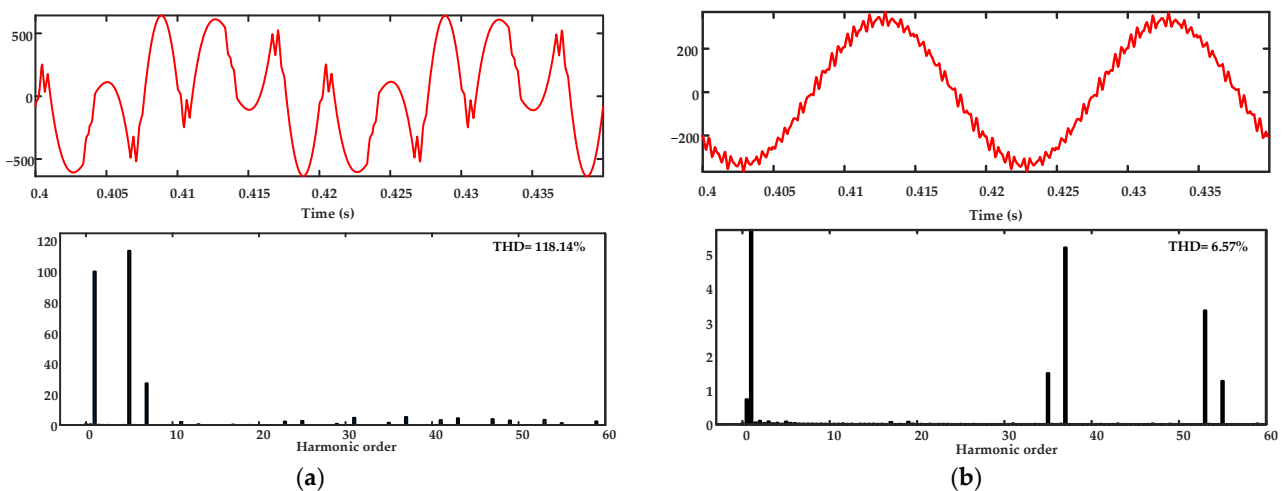


Figure 13. Simulating the current waveform and spectrum in an 18-pulse connection circuit at PPWM with SHE with the 17th and 19th harmonics eliminated: (a) the transformer's secondary winding; (b) grid.

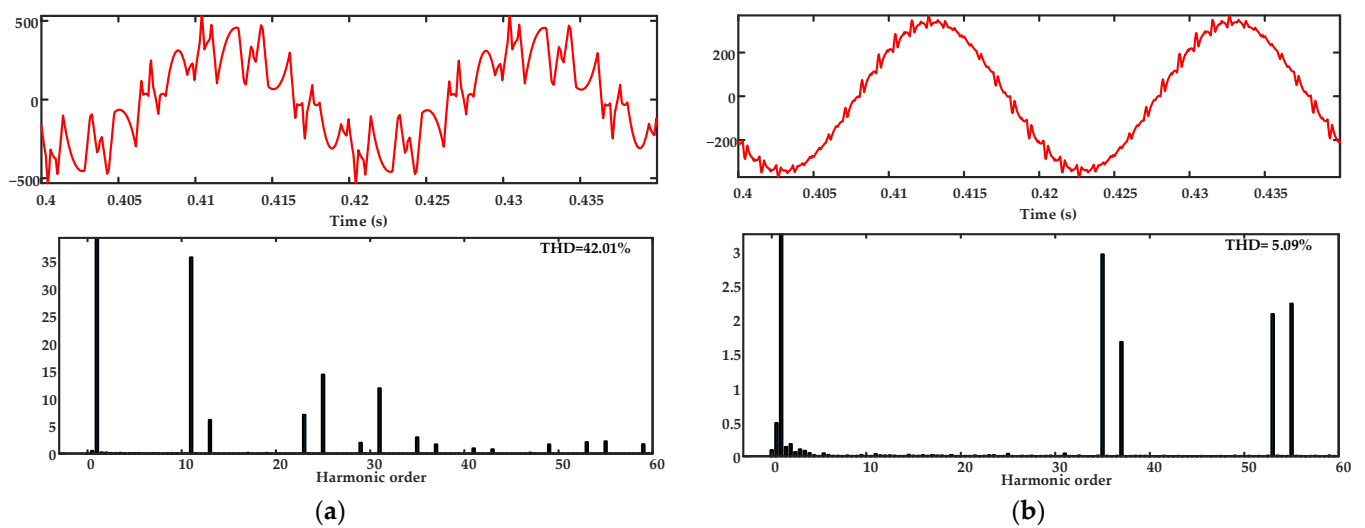


Figure 14. Simulating the current waveform and spectrum in an 18-pulse connection circuit at PPWM with SHE with the 5th, 7th, 17th, and 19th harmonics eliminated: (a) the transformer's secondary winding; (b) grid.

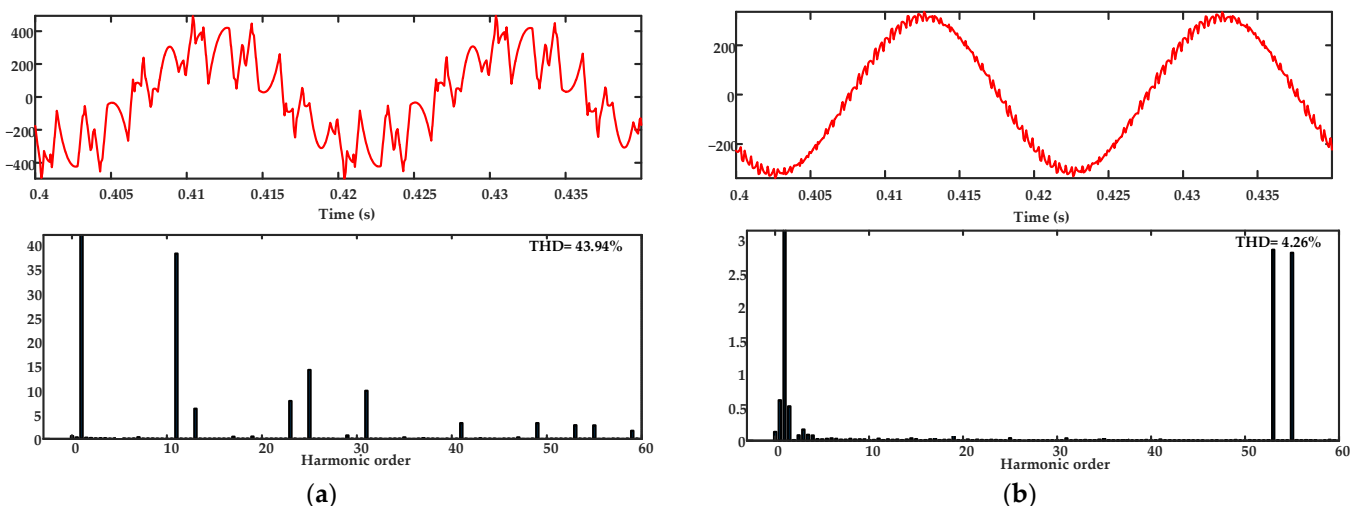


Figure 15. Simulating the current waveform and spectrum in an 18-pulse connection circuit at PPWM with SHE with the 5th, 7th, 17th, 19th, 35th, and 37th harmonics eliminated: (a) the transformer's secondary winding; (b) grid.

Table 4. Comparative analysis of currents in 6-, 12-, and 18-pulse circuits at the modulation index of 1.05.

Connection	Figure Number	PPWM Frequency, Hz	Eliminated Harmonics	THD of Grid Current, %	THD of AFE Current, %
6-pulse	Figure 9a	150	5 and 7	51.92	51.92
	Figure 9b	250	5, 7, 11, and 13	40.23	40.23
	Figure 9c	350	5, 7, 11, 13, 17, and 19	30.26	30.26
12-pulse	Figure 10	150	11 and 13	16.54	113.91
	Figure 11	250	5, 7, 11, and 13	12.44	34.18
	Figure 12	350	5, 7, 11, 13, 23, and 25	9.78	32.96
18-pulse	Figure 13	150	17 and 19	6.57	118.4
	Figure 14	250	5, 7, 17, and 19	5.09	42.01
	Figure 15	350	5, 7, 17, 19, 35, and 37	4.26	43.94

Based on the simulation results, the following conclusions can be drawn:

- (1) As expected, the six-pulse circuit showed the worst grid current THD of 51.92% at the lowest PPWM with SHE frequency of 150 Hz with the elimination of two significant fifth and seventh harmonics (Figure 9a). Increasing the frequency to 250 Hz (Figure 9b) and then 350 Hz (Figure 9c) allowed significantly reducing the grid current THD; however, the results were several times worse than with 12- and 18-pulse circuits. The transformer's secondary winding current simulation results are not provided for a six-pulse connection circuit since the transient process nature is the same as that shown in Figure 9.
- (2) At the PPWM with SHE frequency of 150 Hz with two significant 11th and 13th harmonics eliminated (Figure 10a), a 12-pulse circuit demonstrates a significantly better grid current THD (16.54%) than a 6-pulse one. However, the transformer's secondary winding current THD (Figure 10b) is 113.91%, which is approximately twice as high as with the six-pulse circuit. Note that with an increase in the PPWM with SHE frequency by 100 Hz with additionally eliminated fifth and seventh harmonics, the grid current and the transformer's secondary winding current THDs decreased sharply by 15% and 4 times, amounting to 12.44% (Figure 11a) and 34.18% (Figure 11b), respectively. Increasing the PPWM with SHE frequency up to 350 Hz with the 5th, 7th, 11th, 13th, 23rd, and 25th harmonics eliminated (Figure 12a) expectedly provides the most favorable grid current THD in a 12-pulse circuit; however, the transformer's secondary winding current THD has not changed noticeably (Figure 12b).
- (3) At the PPWM with SHE frequency of 150 Hz with two significant 17th and 19th harmonics eliminated, the 18-pulse circuit, similarly, demonstrates a poor transformer's secondary winding current THD of 118.17% (Figure 13a). However, the grid current THD is only 6.57% (Figure 13b), which is a very good result for a frequency of 150 Hz. With an increase in the PPWM with SHE frequency by 100 Hz with additionally eliminated fifth and seventh harmonics, we can see that the transformer's secondary winding current and the grid current THDs decrease sharply by three times and 15% to 42.01% (Figure 14a) and 5.09% (Figure 14b), respectively. Increasing the PPWM with SHE frequency up to 350 Hz with the 5th, 7th, 17th, 19th, 35th, and 37th harmonics eliminated results in the grid current THD of 4.26% (Figure 15a), which, as expected, is the best result obtained.
- (4) The 18-pulse circuit, other things being equal, allows reducing the grid current THD by two and five-to-seven times compared to the 12-pulse and 6-pulse circuits, respectively.
- (5) Eliminating the fifth and seventh harmonics not only improves the transformer's secondary winding current THD in the 12- and 18-pulse connection circuits but also affects positively the grid current quality.

5. Experimental Results

Theoretical results have been compared with experimental data obtained in the systems of the internal grid of a metallurgical enterprise with powerful AC REDs. The industrial transformer parameters are in Table 5.

Table 5. Transformers parameters.

Grid Connection	S, kVAR	U_1 , V	U_2 , V	I_1 , A	I_2 , A	U_{sc} , %
6-pulse (Figure 3a)	12,000	10,000	3300	693	2189	16
12-pulse (Figure 4)	12,000	10,000	3300	638	1099	14.6

The instantaneous grid current values were recorded using the ELSPEC G4420 power quality analyzer with the possibility of long-term multichannel recording of instantaneous voltage and current values with a high sampling rate. The record sampling rate was 20 kHz. Figures 16 and 17 show the instantaneous grid phase current values and their spectra for

the 6- (Figure 16) and 12-pulse (Figure 17) connection circuits, specifying the THD values calculated for a frequency range from 0 to 3000 Hz (up to the 60th harmonic).

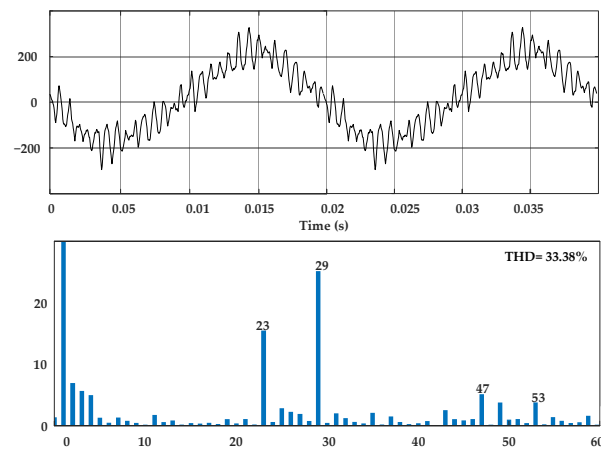


Figure 16. Experimental measurements of the phase current and its spectrum in a 6-pulse grid connection circuit at PPWM with SHE with the 5th, 7th, 11th, 13th, 17th, and 19th harmonics eliminated.

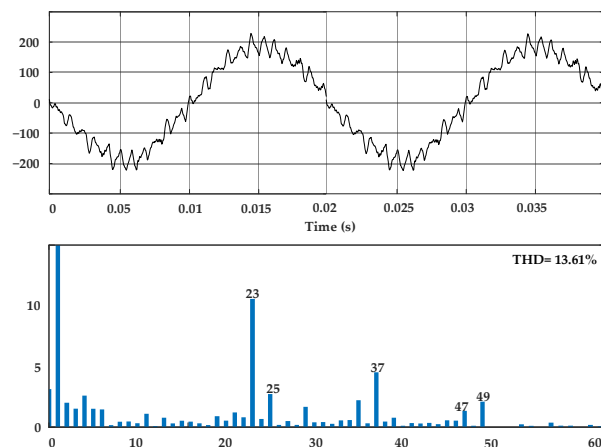


Figure 17. Experimental measurements of the phase current and its spectrum in a 12-pulse grid connection circuit at PPWM with SHE with the 5th, 7th, 11th, and 13th harmonics eliminated.

According to Figure 16, the measured grid current THD value in the six-pulse circuit is 33.38%, which is very close to the simulation results (30.23%, see Figure 9c). An experimental test of the grid current in the 12-pulse circuit in Figure 17 (13.61%) also showed good convergence with similar simulation results (12.44%, see Figure 11b). The mathematical model parameters of the transformers correspond the industrial transformer parameters.

6. Conclusions

The paper's key outcomes and contribution can be summarized as follows:

- (1) The paper reviews the most commonly used grid connection circuits for the main AC REDs of rolling mills. Their advantages and drawbacks, basic components and their characteristics, and three-level AFE's PPWM with SHE algorithms are provided. It is shown that the converters topologies and the PPWM with SHE algorithms should be considered when building the considered power circuits,
- (2) Simulation was performed under the same conditions to objectively estimate and compare the spectra and current THDs of the three-level AFE's 6-, 12-, and 18-pulse connection circuits with various PPWM with SHE algorithms, which was not carried out in previously published studies,

- (3) The comparison results are shown for the powerful AC RED 6-, 12-, and 18-pulse connection circuits with various three-level AFE's PPWM with SHE algorithms. The results can be used to choose the optimal connection circuit and algorithm,
- (4) The experimental data confirm the observations and conclusions provided in this review,
- (5) Based on a literature review, simulation results, and experimental data, recommendations are suggested for choosing PPWM with SHE algorithms for three-level AFEs as part of multi-pulse connection circuits. The results described are of high genericity and can be used by researchers and engineers for designing or performing similar studies in other circuits to provide the electromagnetic compatibility of non-linear consumers.

Author Contributions: Conceptualization, A.S.M.; methodology, A.A.N. and A.S.M.; software, T.J. and A.S.M.; validation, A.A.N.; formal analysis, V.R.G.; investigation, A.A.N. and A.S.M.; resources, A.A.N. and A.S.M.; data curation, A.A.N.; writing—original draft preparation, A.S.M.; writing—review and editing, A.A.N. and T.J.; visualization, A.S.M.; supervision, V.R.G.; project administration, A.S.M. and A.A.N. All authors have read and agreed to the published version of the manuscript.

Funding: 1. This research was funded by Russian Science Foundation, grant number 22-29-20070, <https://rscf.ru/en/project/22-29-20070/> (Sections 1–4 and 6). 2. This research was funded by Russian Science Foundation, grant number 22-19-20069, <https://rscf.ru/en/project/22-19-20069/> (Section 5).

Institutional Review Board Statement: Not applicable.

Informed Consent Statement: Not applicable.

Data Availability Statement: Not applicable.

Conflicts of Interest: The authors declare no conflict of interest.

References

1. Kouro, S.; Malinowski, M.; Gopakumar, K.; Pou, J.; Franquelo, L.G.; Wu, B.; Rodriguez, J.; Pérez, M.A.; Leon, J.I. Recent Advances and Industrial Applications of Multilevel Converters. *Ind. Electron. IEEE Trans.* **2010**, *57*, 2553–2580. [\[CrossRef\]](#)
2. Abu-Rub, H.; Bayhan, S.; Moinoddin, S.; Malinowski, M.; Guzinski, J. Medium-Voltage Drives: Challenges and existing technology. *IEEE Power Electron. Mag.* **2016**, *3*, 29–41. [\[CrossRef\]](#)
3. Rajesh, D.; Ravikumar, D.; Bharadwaj, S.K.; Vastav, B.K.S. Design and control of digital DC drives in steel rolling mills. In Proceedings of the 2016 International Conference on Inventive Computation Technologies (ICICT), Coimbatore, India, 26–27 August 2016. [\[CrossRef\]](#)
4. Abu-Rub, H.; Lewicki, A.; Iqbal, A.; Guzinski, J. Medium Voltage Drives-Challenges and Requirements. In Proceedings of the IEEE International Symposium on Industrial Electronics, Bari, Italy, 4–7 July 2016. [\[CrossRef\]](#)
5. *IEEE Std. 519-1992*; IEEE Recommended Practices and Requirements for Harmonic Control in Electrical Power Systems. IEEE: New York, NY, USA, 1993.
6. *IEEE Std. 1531*; IEEE Guide for Application and Specification of Harmonic Filters. IEEE: New York, NY, USA, 2003.
7. *EN 50160*; Voltage Characteristics of Electricity Supplied by Public Distribution Systems. Wroclaw University of Technology: Wroclaw, Poland, 2001.
8. *IEC 61000-3-2:2019*; Electromagnetic Compatibility (EMC)—Part 3-2: Limits—Limits for Harmonic Current Emissions (Equipment input Current ≤ 16 A per phase). IEC: Geneva, Switzerland, 2019.
9. Kouro, S.; Rodriguez, J.; Wu, B.; Bernet, S.; Perez, M. Powering the Future of Industry: High-Power Adjustable Speed Drive Topologies. *IEEE Ind. Appl. Mag.* **2012**, *18*, 26–39. [\[CrossRef\]](#)
10. Jing, T.; Maklakov, A.S. A Review of Voltage Source Converters for Energy Applications. In Proceedings of the International Ural Conference on Green Energy, Chelyabinsk, Russia, 4–6 October 2018. [\[CrossRef\]](#)
11. Song-Manguelle, J.; Thurnherr, T.; Schroder, S.; Rufer, A.; Nyobe-Yome, J.-M. Re-generative asymmetrical multi-level converter for multi-megawatt variable speed drives. In Proceedings of the 2010 IEEE Energy Conversion Congress and Exposition, Atlanta, GA, USA, 12–16 September 2010. [\[CrossRef\]](#)
12. Rodriguez, J.; Franquelo, L.G.; Kouro, S.; Leon, J.I.; Portillo, R.C.; Prats, M.A.M.; Perez, M.A. Multilevel converters: An enabling technology for high-power applications. *Proc. IEEE* **2009**, *97*, 1786–1817. [\[CrossRef\]](#)
13. Wang, L. *Modeling and Control of Sustainable Power Systems: Towards Smarter and Greener Electric Grids*, 1st ed.; Springer: Hoboken, NJ, USA, 2012.
14. Kornilov, G.P.; Nikolaev, A.A.; Khramshin, T.R. *Mathematical Modeling of the Metallurgical Plants' Electrotechnical Complexes*; Nosov Magnitogorsk State Technical University: Magnitogorsk, Russia, 2012.

15. Mittal, N.; Singh, B.; Singh, S.P.; Dixit, R.; Kumar, D. Multilevel Inverters: A Literature Survey on Topologies and Control Strategies. In Proceedings of the 2nd International Conference on Power, Control and Embedded Systems, Allahabad, India, 1–11 December 2012. [\[CrossRef\]](#)
16. Rodriguez, J.; Bernet, S.; Wu, B.; Pontt, J.O.; Kouro, S. Multilevel voltage-source-converter for industrial medium-voltage drives. *IEEE Trans. Ind. Electron.* **2007**, *54*, 2930–2945. [\[CrossRef\]](#)
17. Franquelo, L.G.; Rodriguez, J.; Leon, J.I.; Kouro, S.; Portillo, R.; Prats, M.A.M. The age of multilevel converters arrives. *IEEE Ind. Electron. Mag.* **2008**, *2*, 28–39. [\[CrossRef\]](#)
18. Ge, B.; Peng, F.Z.; Wu, B.; de Almeida, A.T.; Abu-Rub, H. An effective control technique for medium-voltage high-power induction motor fed by cascaded neutral-point-clamped inverter. *IEEE Trans. Ind. Electron.* **2010**, *57*, 2659–2668. [\[CrossRef\]](#)
19. Ewanchuk, J.; Salmon, J.; Vafakhah, B. A five-/nine-level twelve-switch neutral-point-clamped inverter for high-speed electric drives. *IEEE Trans. Ind. Electron.* **2011**, *47*, 2145–2153. [\[CrossRef\]](#)
20. Bernet, S. State of the art and developments of medium voltage converters—An overview. *Prz. Elektrotechniczny* **2006**, *82*, 1–10.
21. Mohammed, S.A.; Abdel-Moamen, M.A.; Hasanin, B. A review of the state-of-the-art of power electronics for power system applications. *Int. J. Electron. Commun. Eng. Res.* **2013**, *1*, 43–52.
22. Fazel, S.S. *Investigation and Comparison of Multi-Level Converters for Medium Voltage Applications*; Eng.D.-Technische Universität Berlin: Berlin, Germany, 2007.
23. Nabae, A.; Takahashi, I.; Akagi, H. New neutral-point-clamped PWM inverter. *IEEE Trans. Ind. Appl.* **1981**, *IA-17*, 518–523. [\[CrossRef\]](#)
24. Leon, J.I.; Vazquez, S.; Franquelo, L.G. Multilevel converters: Control and modulation techniques for their operation and industrial applications. *Proc. IEEE* **2017**, *105*, 2066–2081. [\[CrossRef\]](#)
25. Abu-Rub, H.; Holtz, J.; Rodriguez, J.; Ge, B. Medium-voltage multilevel converters—State of the art, challenges, and requirements in industrial applications. *IEEE Trans. Ind. Electron.* **2010**, *57*, 2581–2596. [\[CrossRef\]](#)
26. Wu, B.; Narimani, M. *High-Power Converters and AC Drives*, 2nd ed.; Wiley & Sons: Hoboken, NJ, USA, 2017.
27. Singh, B.; Gairola, S.; Singh, B.N.; Chandra, A.; Al-Haddad, K. Multipulse AC–DC Converters for Improving Power Quality: A Review. *IEEE Trans. Power Electron.* **2008**, *23*, 260–281. [\[CrossRef\]](#)
28. Chen, J.; Shen, Y.; Chen, J.; Bai, H.; Gong, C.; Wang, F. Evaluation on the Autoconfigured Multipulse AC/DC Rectifiers and Their Application in More Electric Aircrafts. *IEEE Trans. Transp. Electr.* **2020**, *6*, 1721–1739. [\[CrossRef\]](#)
29. Nikolaev, A.A.; Bulanov, M.V.; Shakhbieva, K.A. Quality Improvement of Electric Power in the Intra-factory Electric Networks through the Use of PWM Algorithm Selective Harmonic Mitigation. In Proceedings of the 2020 Russian Workshop on Power Engineering and Automation of Metallurgy Industry: Research & Practice (PEAMI), Magnitogorsk, Russia, 25–26 September 2020. [\[CrossRef\]](#)
30. Okayama, H.; Uchida, R.; Koyama, M.; Mizoguchi, S.; Tamai, S.; Ogawa, H.; Fujii, T.; Shimomura, Y. Large capacity high performance 3-level GTO inverter system for steel main rolling mill drives. In Proceedings of the IAS '96. Conference Record of the 1996 IEEE Industry Applications Conference Thirty-First IAS Annual Meeting, San Diego, CA, USA, 6–10 October 1996. [\[CrossRef\]](#)
31. De Nazareth Ferreira, V.; Cupertino, A.F.; Pereira, H.A.; Rocha, A.V.; Isaac Seleme, S.; de Jesus Cardoso Filho, B. Design of high-reliable converters for medium-voltage rolling mills systems. In Proceedings of the 2017 IEEE Industry Applications Society Annual Meeting, Cincinnati, OH, USA, 1–5 October 2017. [\[CrossRef\]](#)
32. Bocker, J.; Janning, J.; Jebenstreit, H. High dynamic control of a three-level voltage-source-converter drive for a main strip mill. *IEEE Trans. Ind. Electron.* **2002**, *49*, 1081–1092. [\[CrossRef\]](#)
33. Safaeian, M.; Jalilvand, A.; Taheri, A. A MRAS Based Model Predictive Control for Multi-Leg Based Multi-Drive System Used in Hot Rolling Mill Applications. *IEEE Access* **2020**, *8*, 215493–215504. [\[CrossRef\]](#)
34. Radionov, A.A.; Maklakov, A.S.; Gasiyarov, V.R. Smart Grid for main electric drive of plate mill rolling stand. In Proceedings of the 2014 International Conference on Mechanical Engineering, Automation and Control Systems (MEACS), Tomsk, Russia, 16–18 October 2014. [\[CrossRef\]](#)
35. Pontt, J.A.; Rodriguez, J.R.; Liendo, A.; Newman, P.; Holtz, J.; San Martin, J.M. Network-Friendly Low-Switching-Frequency Multipulse High-Power Three-Level PWM Rectifier. *IEEE Trans. Ind. Electron.* **2009**, *56*, 1254–1262. [\[CrossRef\]](#)
36. Maklakov, A.S.; Radionov, A.A. Integration prospects of electric drives based on back to back converters in industrial smart grid. In Proceedings of the 2014 12th International Conference on Actual Problems of Electronics Instrument Engineering (APEIE), Novosibirsk, Russia, 2–4 October 2014. [\[CrossRef\]](#)
37. Zhang, Y.; Tan, J.; Wang, J.; Li, J. Hardware-in-loop simulation and application for high-power AC-DC-AC rolling mill driving system. In Proceedings of the 2015 IEEE 11th International Conference on Power Electronics and Drive Systems, Sydney, NSW, Australia, 9–12 June 2015. [\[CrossRef\]](#)
38. Nakajima, T.; Suzuki, H.; Izumi, K.; Sugimoto, S.; Yonezawa, H.; Tsubota, Y. A converter transformer with series-connected line-side windings for a DC link using voltage source converters. In Proceedings of the IEEE Power Engineering Society. 1999 Winter Meeting, New York, NY, USA, 31 January–4 February 1999; Volume 2, pp. 1073–1078. [\[CrossRef\]](#)
39. Kornilov, G.P.; Khrashin, T.R.; Abdulveleev, I.R. Increasing stability of electric drives of rolling mills with active front ends at voltage sag. In Proceedings of the 2019 International Conference on Electrotechnical Complexes and Systems (ICOECS), Ufa, Russia, 21–25 October 2019. [\[CrossRef\]](#)

40. Ferreira, V.N.; Cupertino, A.F.; Pereira, H.A.; Rocha, A.V.; Seleme, S.I.; Cardoso, B. Design and Selection of High Reliability Converters for Mission Critical Industrial Applications: A Rolling Mill Case Study. *IEEE Trans. Ind. Appl.* **2018**, *54*, 4938–4947. [\[CrossRef\]](#)
41. Alonso Orcajo, G.; Rodriguez, D.J.; Cano, J.M.; Norniella, J.G.; Ardura, G.P.; Llera, T.R.; Cifrian, R.D. Retrofit of a Hot Rolling Mill Plant with Three-Level Active Front End Drives. *IEEE Trans. Ind. Appl.* **2018**, *54*, 2964–2974. [\[CrossRef\]](#)
42. Espinosa, E.E.; Melin, P.E.; Garcés, H.O.; Baier, C.R.; Espinoza, J.R. Multicell AFE Rectifier Managed by Finite Control Set–Model Predictive Control. *IEEE Access* **2021**, *9*, 137782–137792. [\[CrossRef\]](#)
43. Chengsheng, W.; Chongjian, L.; Chunyi, Z.; Zhiming, L.; Qiongtao, Y.; Wei, D.; Fan, L. Study on large power converter system for rolling mills. In Proceedings of the 2012 15th International Power Electronics and Motion Control Conference (EPE/PEMC), Novi Sad, Serbia, 4–6 September 2012. [\[CrossRef\]](#)
44. Maklakov, A.S.; Jing, T.; Radionov, A.A.; Gasiyarov, V.R.; Lisovskaya, T.A. Finding the Best Programmable PWM Pattern for Three-Level Active Front-Ends at 18-Pulse Connection. *Machines* **2021**, *9*, 127. [\[CrossRef\]](#)
45. Gasiyarov, V.R.; Maklakov, A.S.; Lisovski, R.A. Grid power control by medium voltage AC drives based on back-to-back converters. In Proceedings of the 2018 IEEE Conference of Russian Young Researchers in Electrical and Electronic Engineering (EIConRus), Moscow and St. Petersburg, Russia, 29 January–1 February 2018. [\[CrossRef\]](#)
46. Wang, P.; Liu, F.; Zha, X.; Gong, J.; Zhu, F.; Xiong, X. A Regenerative Hexagonal-Cascaded Multilevel Converter for Two-Motor Asynchronous Drive. *IEEE J. Emerg. Sel. Top. Power Electron.* **2017**, *5*, 1687–1699. [\[CrossRef\]](#)
47. Edpuganti, A.; Rathore, A.K. A Survey of Low Switching Frequency Modulation Techniques for Medium-Voltage Multilevel Converters. *IEEE Trans. Ind. Appl.* **2015**, *51*, 4212–4228. [\[CrossRef\]](#)
48. Jing, T.; Maklakov, A.; Radionov, A.; Baskov, S.; Kulmukhametova, A. Research on hybrid SHEPWM based on different switching patterns. *Int. J. Power Electron. Drive Syst.* **2019**, *10*, 1875–1884. [\[CrossRef\]](#)
49. Edpuganti, A.; Rathore, A.K. A survey of low-switching frequency modulation techniques for medium-voltage multilevel converters. In Proceedings of the 2014 IEEE Industry Application Society Annual Meeting, Vancouver, BC, Canada, 5–9 October 2014. [\[CrossRef\]](#)
50. Veillon, M.; Espinosa, E.; Garcés, H.; Melín, P.; Reyes, M.; Baier, C.; Mirzaeva, G. Feedback Quantizer and Non Linear Control Applied to Multi-Cell AFE Rectifier. In Proceedings of the 2021 IEEE CHILEAN Conference on Electrical, Electronics Engineering, Information and Communication Technologies (CHILECON), Valparaíso, Chile, 6–9 December 2021. [\[CrossRef\]](#)
51. Fernandez-Rebolledo, H.; Sanchez-Ruiz, A.; Ceballos, S.; Perez-Basante, A.; Valera-Garcia, J.J.; Konstantinou, G.; Pou, J. Analysis and Optimization of Modulation Transitions in Medium-Voltage High-Power Converters. *IEEE Trans. Power Electron.* **2021**, *36*, 9984–9993. [\[CrossRef\]](#)
52. Cheng, J.; Xu, T.; Chen, D.; Chen, G. Dynamic and Steady State Response Analysis of Selective Harmonic Elimination in High Power Inverters. *IEEE Access* **2021**, *9*, 75588–75598. [\[CrossRef\]](#)
53. Birth, A.; Geyer, T.; Mouton, H.d.T.; Dorfling, M. Generalized Three-Level Optimal Pulse Patterns with Lower Harmonic Distortion. *IEEE Trans. Power Electron.* **2020**, *35*, 5741–5752. [\[CrossRef\]](#)
54. Jing, T.; Maklakov, A.S.; Radionov, A.A.; Gasiyarov, V.R. Research of a flexible space-vector-based hybrid PWM transition algorithm between SHEPWM and SHMPWM for three-level NPC inverters. *Machines* **2020**, *8*, 57. [\[CrossRef\]](#)
55. Marquez Alcaide, A.; Leon, J.I.; Laguna, M.; Gonzalez-Rodriguez, F.; Portillo, R.; Zafra-Ratia, E.; Vazquez, S.; Franquelo, L.G.; Bayhan, S.; Abu-Rub, H. Real-Time Selective Harmonic Mitigation Technique for Power Converters Based on the Exchange Market Algorithm. *Energies* **2020**, *13*, 1659. [\[CrossRef\]](#)
56. Al-Hitmi, M.; Ahmad, S.; Iqbal, A.; Padmanaban, S.; Ashraf, I. Selective Harmonic Elimination in a Wide Modulation Range Using Modified Newton–Raphson and Pattern Generation Methods for a Multilevel Inverter. *Energies* **2018**, *11*, 458. [\[CrossRef\]](#)
57. Zhang, Y.; Hu, C.; Wang, Q.; Zhou, Y.; Sun, Y. Neutral-Point Potential Balancing Control Strategy for Three-Level ANPC Converter Using SHEPWM Scheme. *Energies* **2019**, *12*, 4328. [\[CrossRef\]](#)
58. Steczek, M.; Jefimowski, W.; Szlag, A. Application of Grasshopper Optimization Algorithm for Selective Harmonics Elimination in Low-Frequency Voltage Source Inverter. *Energies* **2020**, *13*, 6426. [\[CrossRef\]](#)
59. Radionov, A.A.; Gasiyarov, V.R.; Maklakov, A.S.; Maklakova, E.A. Reactive power compensation in industrial grid via high-power adjustable speed drives with medium voltage 3L-NPC BTB converters. *Int. J. Power Electron. Drive Syst.* **2017**, *8*, 1455–1466. [\[CrossRef\]](#)
60. Jing, T.; Maklakov, A.; Radionov, A.; Gasiyarov, V.; Liang, Y. Formulations, Solving Algorithms, Existing Problems and Future Challenges of Pre-Programmed PWM Techniques for High-Power AFE Converters: A Comprehensive Review. *Energies* **2022**, *15*, 1696. [\[CrossRef\]](#)